Modelling Impact-Ionization in the Framework of the Spherical-Harmonics Expansion of the Boltzmann Transport Equation with Full-Band Structure Effects

M. C. Vecchi, M. Rudan

Dipartimento di Elettronica, Università di Bologna,
viale Risorgimento 2, 40136 Bologna, ITALY

Abstract

Band-structure effects have been incorporated in the framework of the Spherical-Harmonics Expansion (SHE) of the Boltzmann Transport Equation (BTE) for electrons in silicon [1], using the density of states (DOS) and the group velocity (GV) obtained from the full-band system [2]. In this paper an impact-ionization model is presented along with the numerical results. The model is consistent with the full-band system mentioned above and is able to fit the impact-ionization coefficient, the impact-ionization quantum yield, and the data from soft x-ray photoemission spettroscopy available in recent literature (e.g., [3]).

1. Physical model

The SHE of the BTE has been tested successfully in a wide range of problems in the field of electron transport simulation [4, 5]. The main advantage of this method is the large dynamic range of its deterministic solution and the ability of predicting the electron distribution, in both the spatially homogeneous and non-homogeneous cases, without the heavy computational burden typical of stochastic methods. Full-band structure effects are incorporated through the DOS and GV independently calculated from the full-band system [2] by means of a suitable averaging procedure. The framework of the SHE method in steady state provides the differential equation [4]

$$
\begin{aligned}
- \;\; & q^2 F^2 \frac{\partial}{\partial E} \left[\tau\, g(E)\, u_g^2(E)\, \frac{\partial f_0}{\partial E} \right] = \\
+ \;\; & 3\, c_{op}\, g(E) \left\{ g^+(E) \left[N_{op}^+ f_0^+(E) - N_{op} f_0(E) \right] - g^-(E) \left[N_{op}^+ f_0(E) - N_{op} f_0^-(E) \right] \right\} \\
- \;\; & 3\, c_{ii}\, g^2(E)\, f_0(E) + 3\, g(E) \int A(E', E)\, f_0(E')\, g(E')\, \mathrm{d}E' .
\end{aligned}
\tag{1}
$$

The symbols have the following meaning: $g(E)$ is the DOS, $u_g(E)$ the modulus of the GV, τ the total scattering rate, F the electric field, c_{op} a constant proportional

to the optical-phonon coupling constant, N_{op} the optical-phonon occupation number, $N_{op}^+ = N_{op} + 1$, $g^{\pm}(E) = g(E \pm \hbar\omega_{op})$, where $\hbar\omega_{op}$ is the optical-phonon energy, and similarly for $f_0^{\pm}(E)$. Impact ionization is also considered: $c_{ii}g(E)$ is the total impact-ionization scattering rate and $A(E', E)$ is a suitable kernel [4]. The non-linear optimization code PROFILE [6] has been used to obtain the best set of scattering parameters by fitting suitable average quantities (mean velocity, energy, impact-ionization coefficient) provided by the Monte Carlo code DAMOCLES [2] and experimental measurements in spatially-homogeneous conditions. The fitting procedure based on the full-band structure, but still using the impact-ionization model of [4], provides the impact-ionization scattering rate shown in Fig. 1. It is seen that the adoption of a full-band structure brings the result of SHE closer to that of Monte Carlo analysis, also shown in the figure. Although the agreement between SHE and Monte Carlo data of Fig. 1 is fair, it can considerably be improved by a sounder description of the impact-ionization mechanism, as shown below.

2. Impact-Ionization model

A three-threshold model is worked out. In order to avoid the simulation of the electrons in the valence band, the latter is assumed flat and full of electrons. The scattering matrix, derived in the Born approximation [7], is:

$$
\begin{aligned}
S^{ii}(\mathbf{k}, \mathbf{k}', \mathbf{k}'') &= \sum_{j=1}^{3} S_j^{ii}(\mathbf{k}, \mathbf{k}', \mathbf{k}'') = \\
&= \sum_{j=1}^{3} b_j^{ii} [a_j^2 + (\mathbf{k}' - \mathbf{k})^2]^{-2}\, \delta(E - E' - E'' - E_{Gj})\,,
\end{aligned}
\tag{2}
$$

where E_{Gj} is the ionization threshold, a_j the inverse screening length, and b_j^{ii} a normalizing constant. The values of the parameters have been determined in order to reproduce the scattering rate presented in [3]. Such scattering rate, in turn, is consistent with the experimental data of [8] and [9]. The scattering rate of [3] is shown in Fig. 2 along with the scattering rate obtained by SHE using 2, while the values of the adopted parameters are reported in Table I.

Table I: impact-ionization model parameters			
Description	Symbol	Value	Unit
Energy threshold	E_{G1}	1.2	eV
Energy threshold	E_{G2}	1.8	eV
Energy threshold	E_{G3}	3.45	eV
Inverse screening length	a_1	5.709×10^7	cm^{-1}
Inverse screening length	a_2	7.032×10^7	cm^{-1}
Inverse screening length	a_3	1.08×10^8	cm^{-1}
Normalization constant	b_1^{ii}	2.96×10^{-5}	cm$^2 \times$eV/sec
Normalization constant	b_2^{ii}	1.04×10^{-3}	cm$^2 \times$eV/sec
Normalization constant	b_3^{ii}	2.92×10^{-1}	cm$^2 \times$eV/sec

It is worth adding that this calculation dealt only with impact ionization, namely, the other parameters mentioned in the previous section have been left unchanged. The impact-ionization coefficient is shown in Fig. 3 and compared with experimental data [10, 11] in a large interval of electric fields: the good agreement in the low-field region

is related to the presence of a soft threshold in (2). Fig. 4 shows the effect of the impact-ionization model on the electron energy-distribution function at 200 kV/cm: the high-energy tail computed with the new model (2) is a few orders of magnitude lower than the one obtained with the old model, due to the higher scattering rate provided by the new model at high energies (compare Figs. 1 and 2). These results emphasize the importance of a correct description of the band structure and impact ionization especially in the analysis of carrier transport at high energies. On the other hand, they also show the ability of the SHE scheme to efficiently incorporate the features of the transport mechanisms to a rather general extent, and reproduce the results of state-of-the-art stochastic methods.

Acknowledgments

References

[1] M. C. Vecchi, D. Ventura, A. Gnudi, G. Baccarani, "Incorporating full band-structure effects in the spherical harmonics expansion of the Boltzmann transport equation," *Proc. of the* NUPAD V *Conf.*, Honolulu, HI, 1994.

[2] M. V. Fischetti, S. E. Laux, *Phys. Rev. B*, "Monte-Carlo analysis of electron transport in small semiconductor devices including band-structure and space-charge effects," vol. 38, pp. 9721–9745, 1988.

[3] E. Cartier, M. V. Fischetti, E. A. Eklund, F. R. McFeely, "Impact Ionization in Silicon," *Appl. Phys. Lett.*, vol. 62, no. 25, 1993.

[4] A. Gnudi, D. Ventura, G. Baccarani, "Modeling Impact Ionization in a BJT by Means of Spherical Harmonics Expansion of the Boltzmann Transport Equation," IEEE *Trans. on* CAD *of* ICAS, vol. 12, no. 11, pp. 1706–1713, 1993.

[5] N. Goldsman, L. Henrickson, J. Frey, "A Physics–Based Analytical/Numerical Solution to the Boltzmann Transport Equation for Use in Device Simulation," *Solid-St. Electr.*, vol. 34, no. 4, p. 389, 1991.

[6] G. J. L. Ouwerling, "Non-destructive Measurament of 2D doping profiles by inverse modelling," *Proc. of the 6th Int.* NASECODE *Conf.*, p. 534, Dublin, 1989.

[7] E. Schöll, W. Quade, "Effect of Impact Ionization on Hot-Carrier Energy and Momentum Relaxation in Semiconductors," *Jour. Physics C*, vol. 20, p. L 861, 1987.

[8] D. J. DiMaria, T. N. Theis, J. R. Kirtley, F. L. Pesavento, D. W. Dong, S. D. Brorson, "Electron heating in silicon dioxide and off-stechiometric silicon dioxide films," *Jour. of Appl. Phys.*, vol. 57, no. 4, p. 1214, 1985.

[9] E. A. Eklund, P. D. Kirchner, D. K. Shuh, F. R. McFeely, E. Cartier, "Direct determination of impact-ionization rates near threshold in semiconductors using soft-x-ray photoemission," *Phys. Rev. Lett.*, vol. 68, no. 6, p. 831, 1992.

[10] R. Van Overstraeten, H. De Man, "Impact ionization of hot electrons in silicon," *Solid-St. Electr.*, vol. 13, pp. 583–608, 1970.

[11] I. Takayanagi, K. Matsumoto, J. Nakamura, "Measuraments of electron impact ionization coefficient in bulk silicon under a low electric field," *J. of Appl. Physics*, vol. 72, no. 5, pp. 1989–1992, 1992.
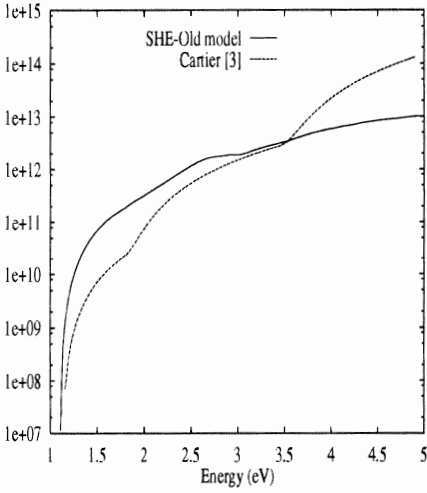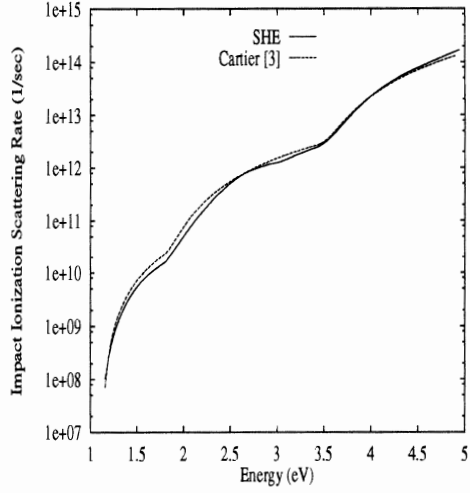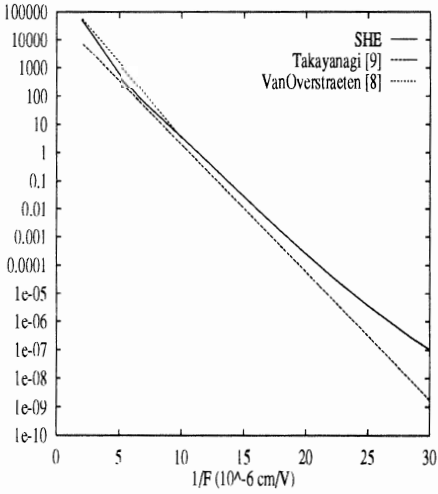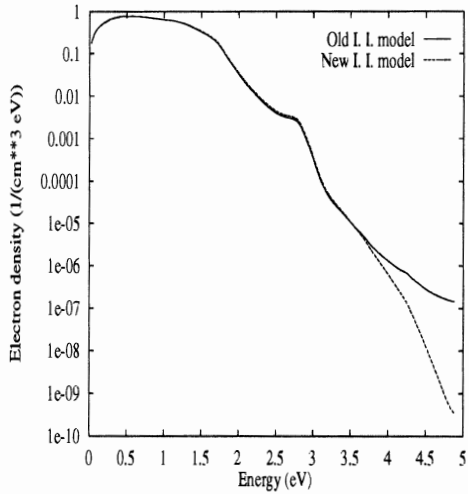
Fig. 1

Fig. 2

Fig. 3

Fig. 4